Nuclear Instruments and Methods in Physics Research A 636 (2011) S104–S110

Contents lists available at ScienceDirect

Nuclear Instruments and Methods in Physics Research A

journal homepage: www.elsevier.com/locate/nima

Evaluation of the bulk and strip characteristics of large area *n*-in-*p* silicon sensors intended for a very high radiation environment

J. Bohm [l,*], M. Mikestikova [l], A.A. Affolder [h], P.P. Allport [h], R. Bates [e], C. Betancourt [m], H. Brown [h], C. Buttar [e], J.R. Carter [b], G. Casse [h], H. Chen [a], A. Chilingarov [g], V. Cindro [i], A. Clark [d], N. Dawson [m], B. DeWilde [o], F. Doherty [e], Z. Dolezal [k], L. Eklund [e], V. Fadeyev [m], D. Ferrere [d], H. Fox [g], R. French [n], C. Garcia [q], M. Gerling [m], S. Gonzalez Sevilla [d], I. Gorelov [j], A. Greenall [h], A.A. Grillo [m], K. Hara [p], H. Hatano [p], M. Hoeferkamp [j], L.B.A. Hommels [b], Y. Ikegami [f], K. Jakobs [c], J. Kierstead [a], P. Kodys [k], M. Köhler [c], T. Kohriki [f], G. Krambergen [i], C. Lacasta [q], Z. Li [a], S. Lindgren [m], D. Lynn [a], P. Maddock [m], I. Mandic [i], S. Marti i Garcia [q], F. Martinez-McKinney [m], R. Maunu [o], R. McCarthy [o], J. Metcalfe [j], M. Mikuz [i], M. Minano [q], S. Mitsui [p], V. O'Shea [e], S. Paganis [n], U. Parzefall [c], D. Puldon [o], D. Robinson [b], H.F.-W. Sadrozinski [m], S. Sattari [m], D. Schamberger [o], S. Seidel [j], A. Seiden [m], U. Soldevila [q], S. Terada [f], K. Toms [j], D. Tsionou [n], Y. Unno [f], J. Von Wilpert [m], M. Wormald [h], J. Wright [m], M. Yamada [p]

[a] Brookhaven National Laboratory, Physics Department and Instrumentation Division, Upton, NY 11973-5000, USA
[b] Cavendish Laboratory, University of Cambridge, JJ Thomson Avenue, Cambridge CB3 0HE, UK
[c] Physikalisches Institut, Universität Freiburg, Hermann-Herder-Street 3, D-79104 Freiburg, Germany
[d] University of Geneva, Switzerland
[e] Department of Physics and Astronomy, University of Glasgow, Glasgow G12 8QQ, UK
[f] Institute of Particle and Nuclear Study, KEK, Oho 1-1, Tsukuba, Ibaraki 305-0801, Japan
[g] Department of Physics, Lancaster University, Lancaster LA1 4YB, UK
[h] Oliver Lodge Laboratory, Department of Physics, University of Liverpool, Oxford St., Liverpool L69 7ZE, UK
[i] Josef Stefan Institute and Department of Physics, University of Ljubljana, Ljubljana, Slovenia
[j] Department of Physics and Astronomy, University of New Mexico, MSC07 4220, 800 Yale Blvd. NE, Albuquerque, NM 87131, USA
[k] Charles University in Prague, Faculty of Mathematics and Physics, V Holesovickach 2, Prague 8, Czech Republic
[l] Academy of Sciences of the CR, Institute of Physics, Na Slovance 2, 18221 Prague 8, Czech Republic
[m] SCIPP, University of California, Santa Cruz, CA 95064, USA
[n] Department of Physics and Astronomy, The University of Sheffield, Hicks Building, Hounsfield Road, S3 7RH Sheffield, UK
[o] Department of Physics and Astronomy, Stony Brook University, Stony Brook, NY 11794-3800, USA
[p] School of Pure and Applied Sciences, University of Tsukuba, 1-1-1 Tennodai, Tsukuba, Ibaraki 305-8571, Japan
[q] IFIC (Centro Mixto CSIC-UVEG), Edificio Investigacion Paterna, Apartado 22085, 46071 Valencia, Spain

ARTICLE INFO

Available online 8 May 2010

Keywords:
Silicon
Micro-strip
ATLAS ID upgrade
SLHC
Leakage current
Depletion voltage
Electrical characteristics
Coupling capacitance
Inter-strip capacitance
Inter-strip resistance

ABSTRACT

The ATLAS collaboration R&D group "Development of *n*-in-*p* Silico*n* Sensors for very high radiation environment" has developed single-sided *p*-type 9.75 cm × 9.75 cm sensors with an *n*-type readout strips having radiation tolerance against the 10^{15} 1-MeV neutron equivalent $(n_{eq})/cm^2$ fluence expected in the Super Large Hadron Collider. The compiled results of an evaluation of the bulk and strip parameter characteristics of 19 new non-irradiated sensors manufactured by Hamamatsu Photonics are presented in this paper. It was verified in detail that the sensors comply with the technical specifications required before irradiation. The reverse bias voltage dependence of various parameters, frequency dependence of tested capacitances, and strip scans of more than 23,000 strips as a test of parameter uniformity and strip quality over the whole sensor area have been carried out at Stony Brook University, Cambridge University, University of Geneva, and Academy of Sciences of CR and Charles University in Prague. No openings, shorts, or pinholes were observed on all tested strips, confirming the high quality of sensors made by Hamamatsu Photonics.

© 2010 Elsevier B.V. All rights reserved.

* Corresponding author. Tel.: +420 266052192; fax: +420 286585443.
E-mail address: bohm@fzu.cz (J. Bohm).

0168-9002/$ - see front matter © 2010 Elsevier B.V. All rights reserved.
doi:10.1016/j.nima.2010.04.093

1. Introduction

The upgrade of the Large Hadron Collider (LHC) to 10 times higher luminosity (10^{35} cm^{-2} s^{-1}), the so-called Super-LHC, will require large changes in design and type of sensors of the current ATLAS Inner Detector (ID). As currently planned, the upgraded ID will consist of silicon sensors: pixel detectors and two types of micro-strip detectors with strip lengths of 2.38 and 9 cm [1]. These micro-strip detectors must withstand an anticipated radiation fluence of up to 5–9 × 10^{14} 1-MeV neutron equivalent (n_{eq})/cm^2 [2].

The ATLAS collaboration R&D group "Development of *n*-in-*p* Silicon Sensors for very high radiation environment" has developed ATLAS07 single-sided *p*-type 9.75 cm × 9.75 cm sensors with an *n*-type readout strips having radiation tolerance against a fluence of 10^{15} n_{eq}/cm^2 [3].

The purpose of this paper is to characterize the ATLAS07 full size sensors and verify the sensor performance required by the Technical Specification [4] before irradiation. The evaluation of irradiated sensors using ATLAS07 miniature samples (1 cm × 1 cm) were studied elsewhere: the bulk damage aspects are reported in Ref. [5] and the surface damages in Ref. [6].

2. ATLAS07 large area sensors

The micro-strip silicon sensors studied in this work are ATLAS07 Series I large area sensors [3] fabricated by Hamamatsu Photonics (HPK) using 6 in. (150 mm) process technology [7]. The baseline is *p*-type float zone silicon with crystal orientation ⟨1 0 0⟩ and a thickness of 320 μm. Sensors are single-sided with capacitively coupled readout *n*-type strips biased through poly-silicon resistors. The readout strips have a pitch of 74.5 μm and are electrically isolated by a common and floating *p*-implant ('*p*-stop' isolation) with a doping concentration of 4 × 10^{12} ions/cm^2. The large area sensor has four segments of strips: Segments 1 and 2 are of axial strips, where the strips are parallel to the edges of the sensor, and Segments 3 and 4 are of stereo strips, where the strips are inclined at an angle of 40 mrad. There are 1280 strips of length 2.38 cm in each segment. Location of four segment areas of the sensor with the strip arrangement and position of DC and AC contact pads is illustrated in Fig. 1. The dead area of the sensor between segments 1 and 2 (3 and 4) and between segments 2 and 3 are 70 and 160 μm broad, respectively.

3. Experimental methods and results

Out of all 30 ATLAS07 Series I large sensors fabricated by HPK, 19 sensors have been measured by the following ATLAS institutes: Academy of Sciences of CR and Charles University in Prague

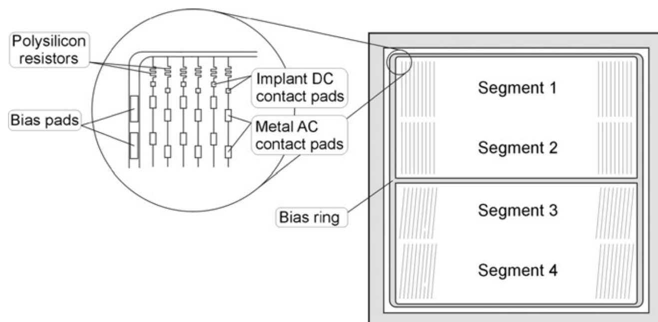

Fig. 1. Location of four segment areas of the ATLAS07 sensor with the strip arrangement and position of DC and AC contact pads (not to scale).

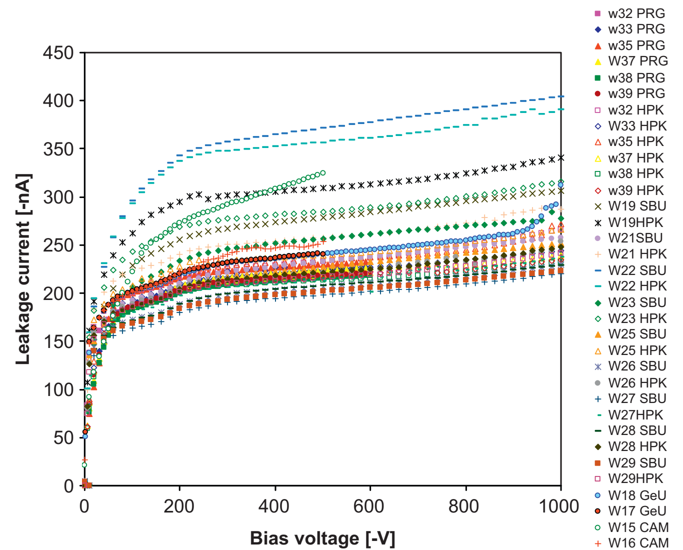

Fig. 2. IV characteristics of large area ATLAS07 Series I sensors normalized to 20 °C.

(sensors W32, W33, W35, W37, W38, W39); Cambridge University (W15, W16); University of Geneva (W17, W18); and Stony Brook University (W19, W21, W22, W23, W25-29).

3.1. Bias voltage and frequency dependence of parameters

3.1.1. Leakage current

The IV characteristics of all 19 tested sensors normalized to 20 °C[1] are shown in Fig. 2. Current was measured with a delay of several seconds (up to 10 s) after setting the reverse bias voltage (V_{bias}). For all tested sensors, the absolute value of the leakage current at 500 V is less than 370 nA. The results are consistent with measurements performed by HPK. The IV characteristics easily comply with the specification [4] that current at 600 V of bias voltage be no greater than 20 μA at 20 °C. Actually, the measured current is more than 50 times lower than this limit.

For most sensors, the IV scan has been measured up to 1000 V. There were no observed onsets of micro-discharges. Sensor W18 had a slow breakdown at ~420 V, but after a short "training," in which the sensor was kept at "breakdown voltage" for a few minutes with current ~10 μA, the breakdown disappeared.

The IV characteristics shown in Fig. 2 were measured before any testing of sensors. The IV scans were repeated after the quality acceptance tests of the sensor (bias voltage scan and strip scan), and the measured leakage current was usually higher by 10–20%.

3.1.2. Bulk capacitance

The bulk capacitance (C_{bulk}) between the backplane and the bias ring as a function of frequency and bias voltage was measured. The frequency dependence measured with function CsRs at 240 V is shown in Fig. 3. One can see that C_{bulk} is constant up to 20 kHz; a frequency of 1 kHz was selected for an estimate of full depletion voltage (FDV).

Plots of the inverse bulk capacitance squared ($1/C^2$) as a function of reverse bias voltage for eight tested sensors are presented in Fig. 4. The full depletion voltages were extracted from the crossing of the linear rise of $1/C^2$ and the saturated plateau.

[1] $I(T_{20})=I(T_M) * (T_{20}/T_M)^2 * \exp[-E/2k_B * (1/T_{20} - 1/T_M)]$ with E = 1.2 eV [8].

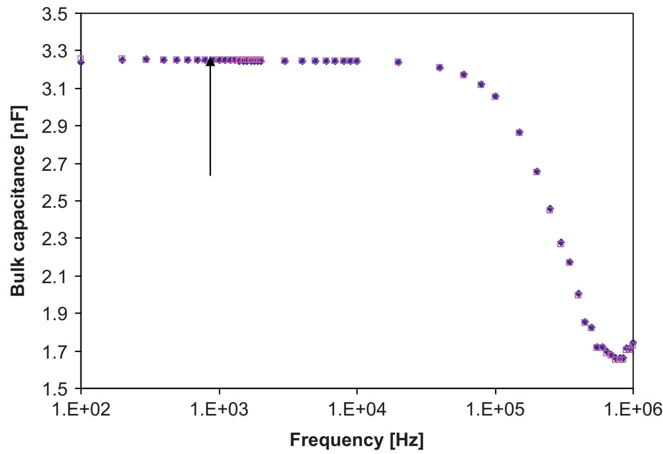

Fig. 3. Frequency dependence of a bulk capacitance of sensors W37 and W38 measured at 240 V.

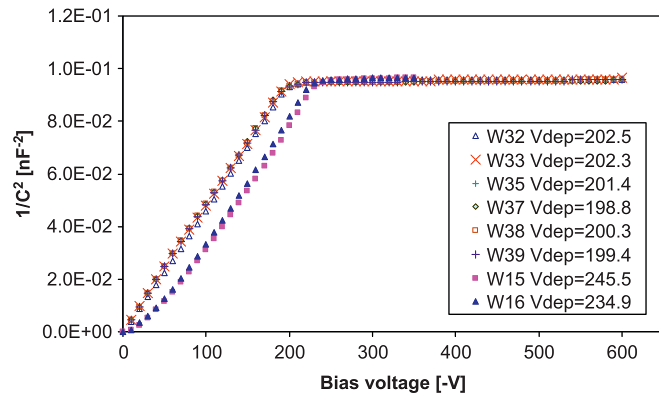

Fig. 4. Bulk capacitance characteristics ($1/C^2$) as a function of bias voltage measured at frequency 1 kHz with CR in series.

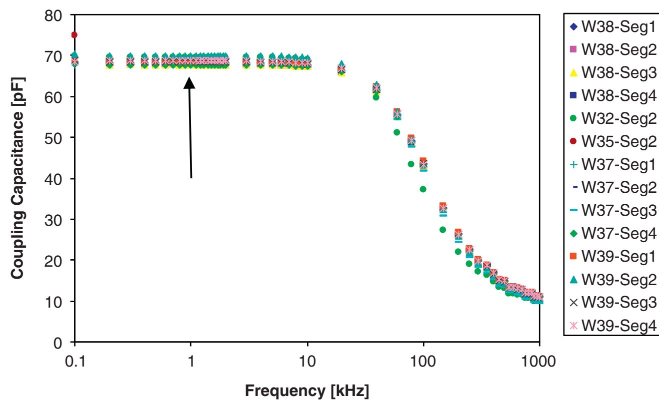

Fig. 5. Frequency dependence of coupling capacitance measured on randomly selected strip from fourteen segments of sensors W32, W35, W37, W38, W39 at reverse bias voltage $V_{bias} = -20$ V with CR in parallel. The frequency 1 kHz has been selected for the bias voltage scan measurement.

All tested sensors reach FDV in the range 199–245 V, which satisfies the Technical Specification requirement of FDV < 500 V.

3.1.3. Coupling capacitance

The coupling capacitance (C_{coupl}) measured between strip metal and strip implant as a function of frequency is shown in Fig. 5. The capacitance is constant up to 10 kHz; beyond 10 kHz, C_{coupl} decreases with frequency. This justifies choosing a frequency of 1 kHz for the bias voltage scan of C_{coupl}.

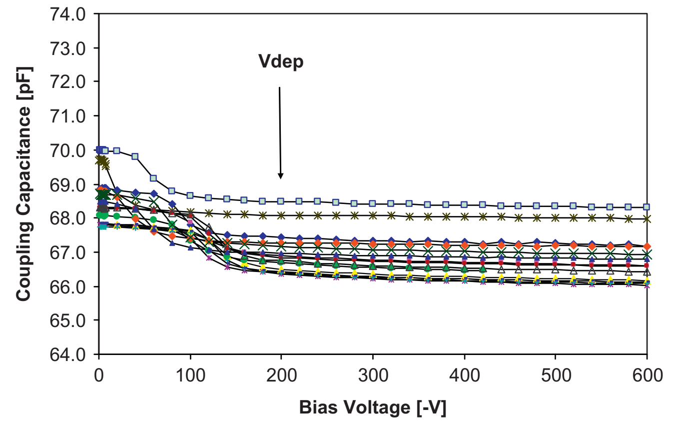

Fig. 6. The coupling capacitance per strip as a function of reverse bias voltage measured at 1 kHz.

The coupling capacitance as a function of bias voltage measured at 1 kHz with CR in parallel is presented in Fig. 6. Beyond full depletion voltage, the C_{coupl} is practically independent of the reverse bias voltage. The values of C_{coupl}/cm achieved are greater than 27.8 pF, which meets the limit $C_{coupl}/\text{cm} > 20$ pF [4].

3.1.4. Bias resistance

The direct method was used for an estimate of the bias resistance. A current–voltage scan was performed applying voltages from 1 to 6 V in 1-V steps to the implant DC pad. The measured implant strip current was a linear function of applied voltage and resistivity was estimated as $R_{bias} = dV_{app}/dI_{meas}$. As expected, the value of the polysilicon bias resistor is not dependent on bias voltage, while the n–p junction is closed (-0.7 V). All measured values were within $R_{bias} = 1.5 \pm 0.5$ MΩ [4].

3.1.5. Inter-strip capacitance

The inter-strip capacitance (C_{int}) contributes dominantly to the input capacitance of FE electronics and determines the noise level of the detector. Therefore, it should be as low as possible. The technical specification [4] defines the upper limit for the inter-strip capacitance as well as the method of measurement: the C_{int}/cm measured between a central metal strip and its nearest neighbors with others floating (three probes) at the 100 kHz test frequency must be less than 1.1 pF/cm.

A better approximation of total C_{int} but more difficult for a measurement is described in Ref. [6]. Five probes are used: three as in the three-probe method and another two probes connecting shield strips to ground. For comparison, randomly selected strips in four segments of W37 were measured with the three- and the five-probe methods. C_{int} (five probes)/C_{int} (three probes) is equal to 0.939 and 0.913 for 100 kHz and 1 MHz test frequency, respectively. One must keep this ratio in mind for a good estimate of noise.

The frequency dependence presented in Fig. 7 shows that the three-probe inter-strip capacitance is in fact saturated at 1 MHz and not at 100 kHz, contrary to the five-probe C_{int} which plateaus at about 100 kHz. From the above statement, one can suggest the frequency of 1 MHz instead of 100 kHz for the three-probe method in the technical specification. The reverse bias voltage dependence of C_{int} measured by the three- and five-probe methods is shown in Fig. 8. C_{int} becomes constant beyond FDV

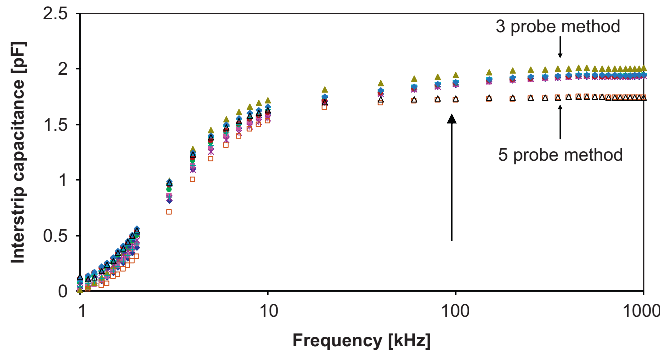

Fig. 7. Frequency dependence of inter-strip capacitance measured with three-probe method (full symbols) and with five-probe method (open symbols) at $V_{bias}=240$ V.

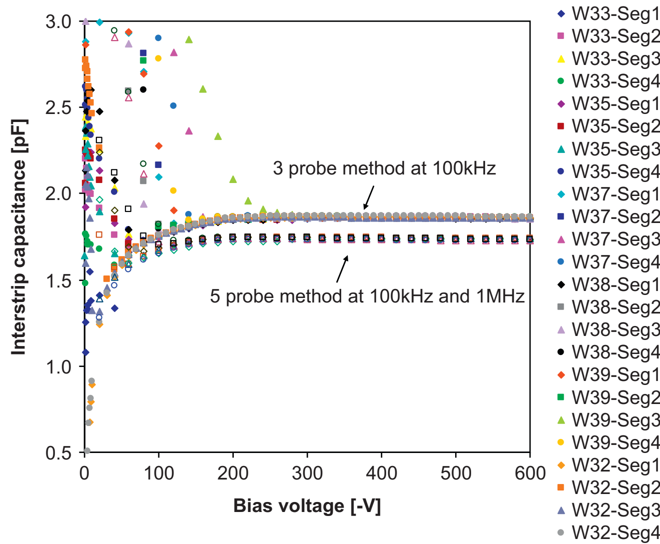

Fig. 8. Inter-strip capacitance as a function of the reverse bias voltage measured at randomly selected strips from each segment with the three-probe method at 100 kHz (full symbols) and with the five-probe method (open symbols) at 100 kHz and 1 MHz test frequencies.

for all tested sensors and segments. The C_{int} values measured by the three-probe method at 100 kHz test frequency are in the interval 0.75–0.80 pF/cm, in agreement with the specification.

The five-probe results at 100 kHz and at 1 MHz are also displayed in Fig. 8 (open symbols). C_{int} values are the same for both frequencies.

3.1.6. Inter-strip resistance

The *p*-stop isolation between neighboring strips is well demonstrated by the inter-strip resistance (R_{int}) values. Inter-strip resistance was measured by contacting three adjacent implant DC pads with three probes [9,10]. A voltage, U_{app}, was applied to the outer strips in the interval (−5 V, +5 V) with a step of 1 V. The current was measured on the central DC pad. The inter-strip resistance was calculated as

$$R_{int}=2/(dI/dU_{appl}).$$

Inter-strip current is directly proportional to applied voltage, as shown in Fig. 9, and inter-strip resistance is independent of bias voltage, as shown in Fig. 10. The measured values of R_{int} for all tested sensors are in the range 150–600 GΩ/cm, and thus comply with the Technical Specification: $R_{int}>10\times R_{bias}\sim 15$ MΩ.

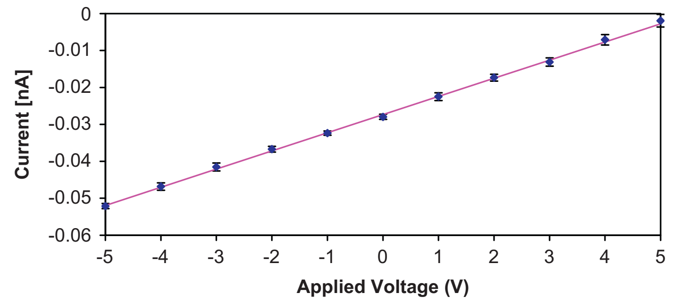

Fig. 9. Inter-strip current as a function of applied voltage for sensor W23.

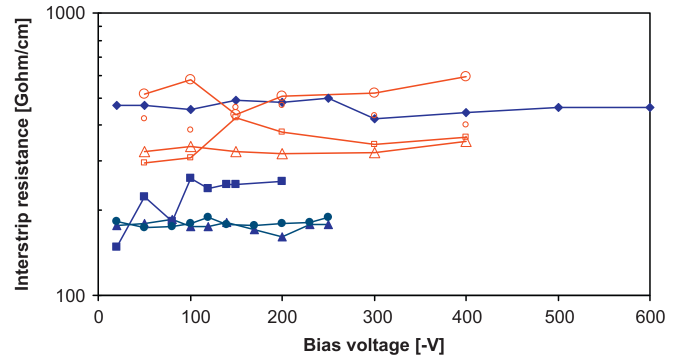

Fig. 10. Inter-strip resistance per centimeter as a function of reverse bias voltage for sensor W37 (full symbols) and W38 (open symbols) measured on arbitrary strips from each segment.

3.2. Strip scans

3.2.1. Measurement techniques

The aim of strip-to-strip measurements is to study strip integrity and uniformity of electrical characteristics over the whole sensor. It requires probing 1280 strip pads on each of four sensor segments. To keep the time involved to a reasonable limit, simplified measurement techniques were used which are not as precise as the ones used for bias voltage scans (see the previous Section 3.1). Inter-strip resistance was measured between two DC pads only, and coupling capacitance and bias resistance were measured by the CSRS function at 100 kHz between the metal strip and the bias ring. A switching matrix was used to perform multiple tests on adjacent strips using an automatic probe station. Two needles probing two AC pads on the metal strips were used for measurement of C_{coupl}, R_{bias}, and current through the coupling dielectric, while four needles probing two AC pads and two DC pads of neighboring strips were used for measurement of R_{int} and I_{strip}. For better accuracy, the inter-strip capacitance was measured by the three-probe method and without the switching matrix.

3.2.2. Bias resistance and coupling capacitance

Measurements of coupling capacitance and bias resistance were performed on 18 segments of five sensors, a total of 23,040 strips. An example of the bias resistance measurement is shown in Fig. 11(a) together with the R_{bias} distribution given in Fig. 11(b). One can recognize small differences between segments, which can be characterized by FWHM=120 kΩ of the R_{bias} distribution. The results measured on all other sensors are similar. The values of bias resistors are uniform and in the range of 1.5±0.5 MΩ as required by the specifications.

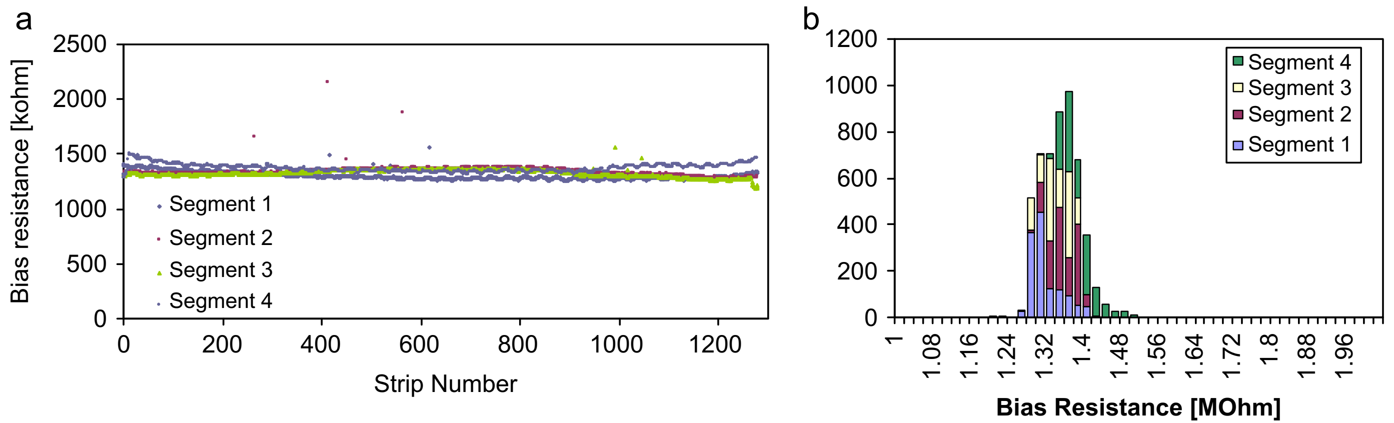

Fig. 11. (a) Bias resistances and (b) R_{bias} distribution of sensor W23.

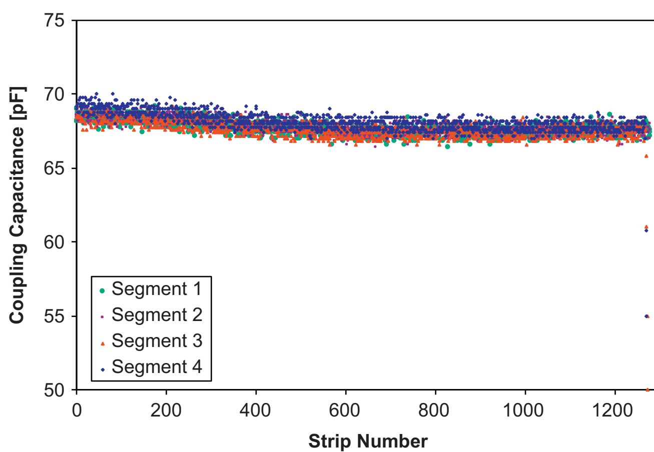

Fig. 12. Coupling capacitance versus strip number for sensor W15.

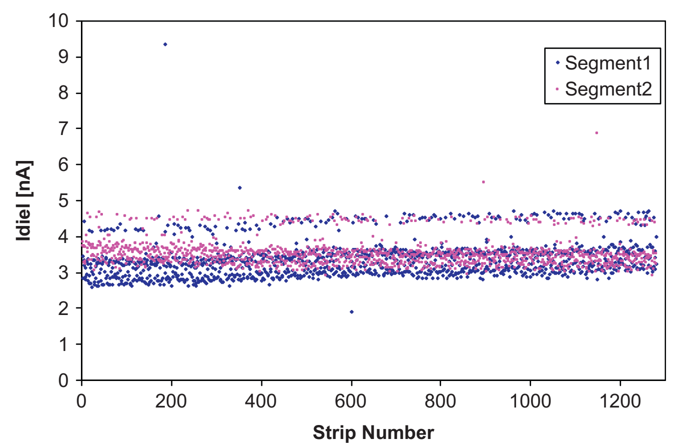

Fig. 13. Measurement of current through the coupling dielectric for two segments of W38.

The measurement of coupling capacitance probes strip defects, such as an opening in a metal strip for which C_{coupl} is smaller than average and a short between two adjacent metal or implant strips for which C_{coupl} is about two times greater than for a single strip.

No openings or shorts were observed on all 23,040 tested strips, confirming the high quality of sensors made by HPK. An example of the coupling capacitance measurements across an entire sensor is given in Fig. 12. Small differences between segments can be described by FWHM of the C_{coupl} distribution that is equal to 1.5 pF. Lower capacitances near the edges of Segments 3 and 4 were expected due to the geometry of the inclined strips. The measured values of C_{coupl} comply with specifications.

3.2.3. Current through the coupling dielectric

The current flowing through the coupling dielectric (I_{diel}) was measured at 100 V applied to the AC pad. The measured values of I_{diel} for two segments of sensor W38 are shown in Fig. 13. The I_{diel} for all 12,800 tested strips is less than ~10 nA. Thus, there are no pinholes or punch-through defects in the coupling dielectric of tested sensors.

3.2.4. Strip current

Strip current (I_{strip}) was measured between the DC pad on an implant strip and the ground of a fully depleted sensor. I_{strip} probes the bulk and implant homogeneity. The measured strip current was smaller than 2 nA for all 10,240 tested strips; results for sensor W23 are shown in Fig. 14. There are about 60 strips in segments 2 and 3 with significantly higher I_{strip}, but which is still less than 2 nA. In the same strip region, a weaker signal is also observed in the conductance distribution (see Fig. 17). The origin of this non-uniformity is not known.

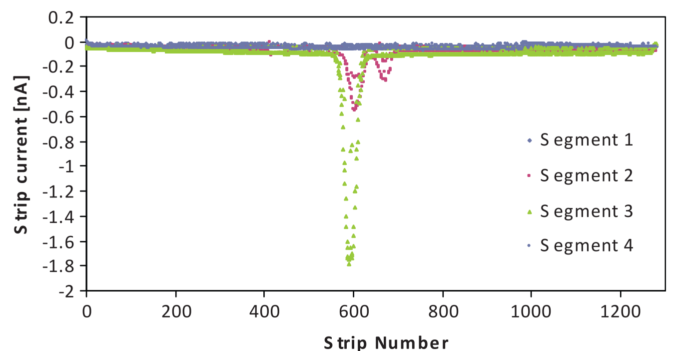

Fig. 14. Strip current measured for sensor W23.

3.2.5. Inter-strip capacitance and resistance

Inter-strip capacitance was measured on four segments of sensor W37 by the three-probe method at 100 kHz test frequency and V_{bias}=240 V, yielding 2560 values of C_{int} (see Fig. 15). The C_{int}

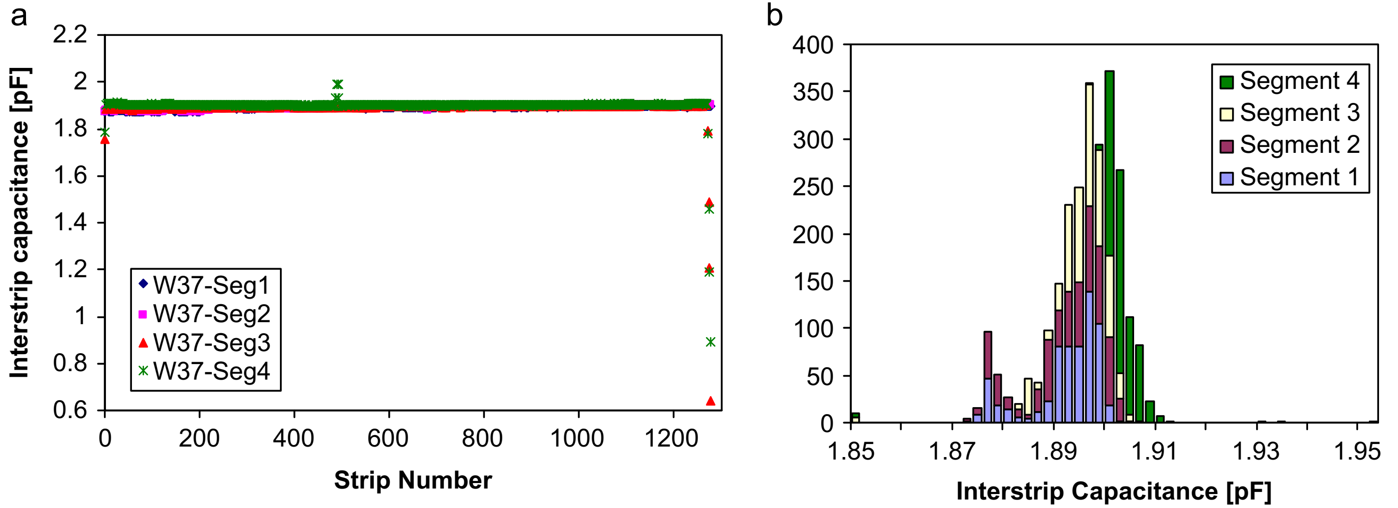

Fig. 15. (a) The inter-strip capacitance measurement with the three-probe method and (b) C_{inter} distribution for sensor W37.

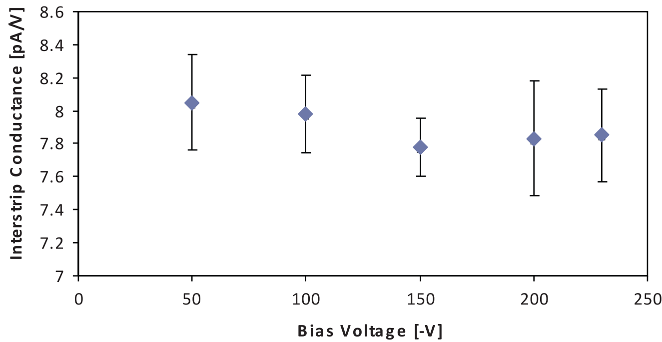

Fig. 16. Inter-strip conductance ($Cond_{int}=1/R_{int}$) as a function of bias voltage for sensor W25.

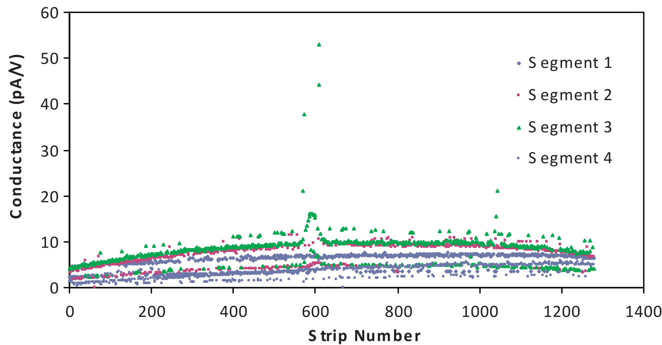

Fig. 17. The inter-strip conductance measured on pair of strips of sensor W23.

distribution given in Fig. 15(b) is characterized by FWHM = 12 fF which confirms good parameter uniformity over the whole sensor.

The first and last few stereo strips on Segments 3 and 4 are shorter; consequently, the measured C_{int} is significantly decreased, as is visible in Fig. 15(a). There are four observed values of C_{int}, which are higher by ~100 fF than others on Segment 4 and a jump by ~20 fF on Segments 1 and 2 near strip number 500.

The average value of C_{int} is 1.895 pF, which is ~30 fF above the average value of 1.866 pF measured during the bias voltage scan. This small difference is presumably due to the decrease of C_{int} in time at higher relative humidity (RH was ~30%) during the slow bias voltage scan [11].

Table 1
Comparison of measured parameter values with technical specification [4].

	ATLAS07 specification	Measurement
Leakage current	< 20 μA at 600 V	200 nA–370 nA
Full depletion voltage	< 500 V	190 V–245 V
Coupling capacitance at 1 kHz	> 20 pF/cm	> 28 pF/cm
Silicon bias resistance	1.5 ± 0.5 MΩ	1.3–1.6 MΩ
Current through dielectric	I_{diel} < 10 nA Pinhole: $I_{diel} \gg 10$ nA	< 10 nA
Strip current	No explicit limit	< 2 nA
Inter-strip capacitance	< 1.1 pF/cm	
3 probe method 100 kHz		0.7 pF/cm–0.8 pF/cm
5 probe method		0.66 pF/cm–0.75 pF/cm[a]
Inter-strip resistance per cm	> 10 × R_{bias} ~ 15 MΩ	> 150 GΩ

[a] For a noise estimate the five-probe method should be used (see Section 3.1.5).

The inter-strip resistance (R_{int}) has been measured on a pair of strips of a fully depleted sensor: A voltage of ±10 V was applied to the DC pad of the first implant strip and current to ground was measured on the second strip. Conductance is defined as dI/dV, and $R_{int}=1/conductance$. As a test of this method, the reverse bias voltage dependence of the inter-strip conductance was measured on arbitrary pair of strips (see Fig. 16). There is no dependence on bias voltage, as expected, and the average conductance of 7.9 pA/V corresponds to R_{int}/cm = 300 GΩ.

Inter-strip conductance for all pairs of strips of sensor W23 is displayed in Fig. 17. With the exception of four pairs in the center of the sensor, the measured inter-strip conductance is smaller than 15 pA/V. This corresponds to R_{int}/cm > 150 GΩ, in compliance with the technical specification. Similar results were obtained for sensor W25. Consequently, one can conclude that a common *p*-stop with doping concentration of 4×10^{12} *ions*/cm^2 provides acceptable electrical isolation of *n*-type strips.

4. Summary

The results of measurements and comparison of values to the ATLAS07 specification are summarized in Table 1.

5. Conclusions

An evaluation of 19 ATLAS07 Series I large area sensors manufactured by Hamamatsu Photonics has been presented. All tested sensors satisfied Technical Specification of non-irradiated sensors for leakage current and full depletion voltage as well as for coupling capacitance, bias resistance, inter-strip capacitance and resistance measured with the bias voltage scan. The onset voltage of micro-discharges for ATLAS07 large area sensors is $V_{\mathrm{MD}} > 1000$ V.

Strip scans were performed on six sensors. Measurements of coupling capacitance and the current through the coupling dielectric show that there are no defects (shorts or openings of metal strips) on the 23,040 tested strips. Measurements of coupling capacitance and bias resistance on one strip as well as measurements on pairs of strips of the inter-strip resistance and the three-probe measurement of C_{int} confirmed no systematic deviations from uniform distributions. However, the test of the strip current of sensor W23 showed non-uniformity for about 60 strips in the center of sensor. All evaluated sensors passed the tests of quality acceptance.

Acknowledgements

We would like to express our thanks to K. Yamamura and S. Kamada of Hamamatsu Photonics K.K. for helpful comments on the design of the sensor.

The authors acknowledge the support of the funding authorities of the collaborating institutes, including the Ministry of Education, Youth and Sports of the Czech Republic (Grant no. LA 08032), the German Federal Ministry of Education and Research, the Japan Grant-in-Aid for Scientific Research (A) (Grant no. 20244038), Research (C) (Grant no. 20540291) and Research on Priority Area (Grant no. 20025007), the Slovenian Research Agency, the Spanish National Program for Particle Physics, the U.S. Department of Energy, the U.S. National Science Foundation (under Grant PHY0652607), and the U.K. Science and Technology Facilities Council (under Grant PP/E006701/1).

References

[1] P.P. Allport, Nucl. Instr. and Meth. A 579 (2007) 592.
[2] I. Dawson, Radiation predictions at the SLHC and irradiation facilities, in ATLAS Tracker Upgrade Workshop, Liverpool, 6–8 December 2006, http://www.liv.ac.uk/physics/AHLUTW/.
[3] Y. Unno et al., Development of *n*-on-*p* silicon sensors for very high radiation environment, this issue.
[4] S.C.T. ATLAS Collaboration, Technical specification: Supply of Silicon Micro-strip Sensors of ATLAS07 specification, 7th October 2007, 〈https://edms.cern.ch/file/888375/2/ATLAS07TechnicalSpecR4.6.pdf〉.
[5] K. Hara et al., Testing of bulk radiation damage of *n*-in-*p* silicon sensors for high radiation environments, this issue.
[6] S. Lindgren et al., Testing of surface properties pre-rad and post-rad of *n*-in-*p* silicon sensor for very high radiation environment, this issue.
[7] Hamamatsu Photonics K.K., 1266 Ichino-cho, Hamamatsu-shi 435-8558, Japan.
[8] H.F.-W. Sadrozinski, personal communication.
[9] H.F.-W. Sadrozinski, Status of strip detectors, in ATLAS meeting at UC Santa Cruz, http://scipp.ucsc.edu/ATLAS%20Mtg_2008/.
[10] A. Chilingarov, RD50 recommendations towards a standardisation of the macroscopic parameter measurements https://rd50.web.cern.ch/rd50/doc/recommendations.html.
[11] A. Chilingarov, Nucl. Instr. and Meth. A 560 (2006) 118.